A density functional theory study on size-dependent structures, stabilities, and electronic properties of bimetallic $M_n\mathrm{Ag}_m$ (M=Na, Li; $n+m \leq 7$) clusters*

Sun Hao-Ran(孙浩然), Kuang Xiao-Yu(邝小渝)†, Li Yan-Fang(李艳芳), Shao Peng(邵 鹏), and Zhao Ya-Ru(赵亚儒)

Institute of Atomic and Molecular Physics, Sichuan University, Chengdu 610065*, China*

(Received 24 October 2011; revised manuscript received 16 November 2011)

The equilibrium geometries, relative stabilities, and electronic properties of $M_n\mathrm{Ag}_m$(M=Na, Li; $n+m \leq 7$) as well as pure Ag_n, Na_n, Li_n ($n \leq 7$) clusters are systematically investigated by means of the density functional theory. The optimized geometries reveal that for $2 \leq n \leq 7$, there are significant similarities in geometry among pure Ag_n, Na_n, and Li_n clusters, and the transitions from planar to three-dimensional configurations occur at $n = 7$, 7, and 6, respectively. In contrast, the first three-dimensional (3D) structures are observed at $n + m = 5$ for both $\mathrm{Na}_n\mathrm{Ag}_m$ and $\mathrm{Li}_n\mathrm{Ag}_m$ clusters. When $n + m \geq 5$, a striking feature is that the trigonal bipyramid becomes the main subunit of $\mathrm{Li}_n\mathrm{Ag}_m$. Furthermore, dramatic odd–even alternative behaviours are obtained in the fragmentation energies, second-order difference energies, highest occupied and lowest unoccupied molecular orbital energy gaps, and chemical hardness for both pure and doped clusters. The analytic results exhibit that clusters with an even electronic configuration (2, 4, 6) possess the weakest chemical reactivity and more enhanced stability.

Keywords: $M_n\mathrm{Ag}_m$ (M=Na, Li) clusters, density functional theory, relative stability

PACS: 36.20.Hb, 36.40.–c, 36.40.Qv **DOI:** 10.1088/1674-1056/21/8/083601

1. Introduction

As a bridge between molecular and condensed matter physics, clusters usually show particular and interesting properties which are different from their extended bulk and atomic states. Among small-size clusters, bimetallic and pure clusters have been most extensively investigated, owing to the motivation of designing novel nanofunctional materials, which are applied in fields such as optics, catalysis, and nanotechnology.[1−8] Furthermore, in the bimetallic and pure cluster science, "*s*-simple" alkali-metal becomes a hot research object.[9−16] Interestingly, it is worth noting that the electronic shell model is suitable for the small-size clusters of noble metals, for the noble metal atoms have a similar electronic configuration of nd^{10} $(n+1)s^1$ to that of alkali-metal.[17,18] During the last decades, coinage-alkali metal clusters have attracted much attention,[19−23] as the addition of heteroatoms to clusters can dramatically affect the equilibrium geometries and physical–chemical properties of the host nanoparticles.

Recently, two electronic systems: NaAg and LiAg, have been observed with resonant photoionization spectroscopy and pulsed supersonic molecular beam by laser vaporization, and their bond lengths, vibrational frequencies and dissociation energies are obtained.[24,25] Meanwhile, by combining valence-bond photoemission and Ag (MVV) Auger spectra on lithium silver alloys, Rodriguez and Hrbek[26] reported that the Ag–Li bond is mainly metallic with a small degree of ionic character. Subsequently, with the density functional theory (DFT), Wannere *et al.*[27] demonstrated that for the doubly bridged square planar (D_{4h}) $\mathrm{Ag}_4\mathrm{Li}_2$ cluster, the delocalization of *d* and to some extent *s* orbitals play a main role in its cluster bonding. Also the nonscalar relativistic effects are found to be a dominant effect on the excited state of CsAg by theoretical investigation.[28] Later on, Lin *et al.*[29] applied the DFT to the study of structures of $\mathrm{Ag}_4\mathrm{Li}^-$ and $\mathrm{Ag}_4\mathrm{Na}^-$ clusters and concluded that the pyramidal isomers have the lowest-energy structures. In addition, systematic calculations based on

*Project supported by the Doctoral Education Fund of the Education Ministry of Chain (Grant No. 20100181110086) and the National Natural Science Foundation of China (Grant Nos. 11104190 and 10974138).

†Corresponding author. E-mail: scu_kuang@163.com

© 2012 Chinese Physical Society and IOP Publishing Ltd

BPW91/LANL2DZ method showed prominent peaks at NaAg, Na_7Ag, and Na_9Ag within the Na_nAg series, indicating that electronic shell closures determine the stability of these clusters.[30]

Up to now, many studies have been devoted to coinage-alkali metal clusters, however, to the best of our knowledge, few systematic investigations on mixed Na–Ag and Li–Ag bimetallic clusters have been performed. In the present work, we calculate equilibrium geometries, atomic average binding energies, fragmentation energies, second-order difference of energies, HOMO–LUMO (highest occupied molecular orbital–lowest unoccupied molecular orbital) energy gaps and chemical hardness, for M_nAg_m (M=Na, Li; $n+m \leq 7$) clusters and pure frameworks. It is hoped that our studies can supply a vivid image of M_nAg_m clusters.

The rest of the present paper is organized as follows. In Section 2, the computational method is briefly outlined. In Section 3, the results are presented and discussed. Finally, the conclusions are drawn from the present study in Section 4.

2. Computational method

In this paper, we conduct geometry optimizations, together with the frequency analysis of the M_nAg_m (M=Na, Li; $n+m \leq 7$) at the level of Becke's 1988 exchange functional with Perdew's gradient-corrected correlation functional method (BP86).[31,32] As the calculations concerning full electrons are rather time-consuming due to the heavy Ag atom, it is necessary to introduce the effective core potential including the relativistic effect (RECP) to describe the inner-core electrons. Under this approximation, the basis set denoted with GENECP is the combination of the LanL2DZ[33−35] for Ag and 6-311G* for Na/Li. All calculations are performed using the GAUSSIAN 03 program package.[36]

In order to check the validity of the computational method, we make a test by employing different basis sets and density functions for the small Na–Ag and Li–Ag clusters. The results are shown in Table 1. As seen in Table 1, it is easy to find that the results based on the BP86 density function and LanL2DZ basis set are well consistent with the experimental data.[24,25] This result indicates that the computational method we have chosen is suited to describe the small-size M_nAg_m (M=Na, Li; $n+m \leq 7$) clusters. To determine the lowest-energy structure, lots of possible initial structures at various spin multiplicities have been extensively explored in geometry optimizations. Meanwhile, vibration frequency calculations have been carried out to provide zero-point energy (ZPE) and guarantee that the optimized structure corresponds to a local minimum of energy.

Table 1. Ground-state properties of NaAg and LiAg based on different sets and density functions, 1 Å=0.1 nm.

Basis set	Density function	NaAg			LiAg		
		r/Å	ω/cm^{-1}	D_e/eV	r/Å	ω/cm^{-1}	D_e/eV
SDD	B3LYP	2.68	206.93	1.52	2.38	370.50	1.81
	B3PW91	2.69	205.88	1.39	2.40	368.95	1.67
	PW91PW91	2.67	210.00	1.69	2.37	376.46	1.96
	B3P86	2.67	210.73	1.53	2.37	376.56	1.83
	BP86	2.67	209.81	1.65	2.37	377.23	1.96
	BPW91	2.69	207.20	1.51	2.38	373.20	1.79
LanL2DZ	B3LYP	2.67	207.39	1.52	2.38	370.11	1.80
	B3PW91	2.68	206.37	1.38	2.40	366.57	1.65
	PW91PW91	2.68	210.95	1.67	2.40	378.47	1.94
	B3P86	2.67	210.54	1.53	2.38	375.56	1.82
	BP86	2.67	210.59	1.62	2.37	378.57	1.91
	BPW91	2.68	208.56	1.48	2.38	373.44	1.77
	Experiment	–	210.00[24]	$\geqq$ 1.59[24]	2.41±0.02[25]	389.00[25]	1.89±0.004[25]

3. Results and discussion

3.1. Equilibrium geometry

To compare the effects of doped impurity atoms on the bare clusters, we first performed some geometric optimizations for bare Ag_n, Na_n, and Li_n (n = 2–7) clusters using the identical theoretical method and basis set. The lowest-energy structures at each cluster size are respectively presented in Figs. 1 and 2. One can find that except for n = 6, the lowest-energy struc-

tures of pure Ag_n, Na_n, and Li_n clusters have similar configurations, with their sizes being identical. It is worth pointing out that the calculated ground-state configurations and growing patterns of Ag_n clusters are exactly consistent with those in Ref. [37].

3.1.1. Geometries and growth pattern behaviours of Na_nAg_m

During the period of studying M_nAg_m (M=Na, Li; $n+m \leq 7$) clusters, a large number of possible initial structures have been obtained, but here only the most stable isomers are selected from among those isomers for each size as shown in Figs. 1 and 2, and the corresponding electronic states and geometric symmetries are also listed there. We can easily find that the geometries of the ground-state pure and bimetallic M_nAg_m isomers are all singlet for isomers with even-numbered atoms while doublet for clusters with odd-numbered ones.

Analysing $NaAg_m$ (m = 1–6) clusters in Fig. 1, the most stable $NaAg_m$ isomers can be obtained by replacing one Ag atom in pure silver clusters, and the silver frameworks are almost unchanged in the presence of the Na atom (except $NaAg_2$). In the case of the ground-state C_{2v} $NaAg_2$ cluster, the cluster forms an acute triangle structure with a bending angle of 59.58° between Ag–Na–Ag, while Ag_3 structure has a bending angle of 143.57°, and the Ag–Na bond length of $NaAg_2$ (2.81 Å, 1 Å=0.1 nm) is slightly longer than the Ag–Ag bond length (2.65 Å) of Ag_3.

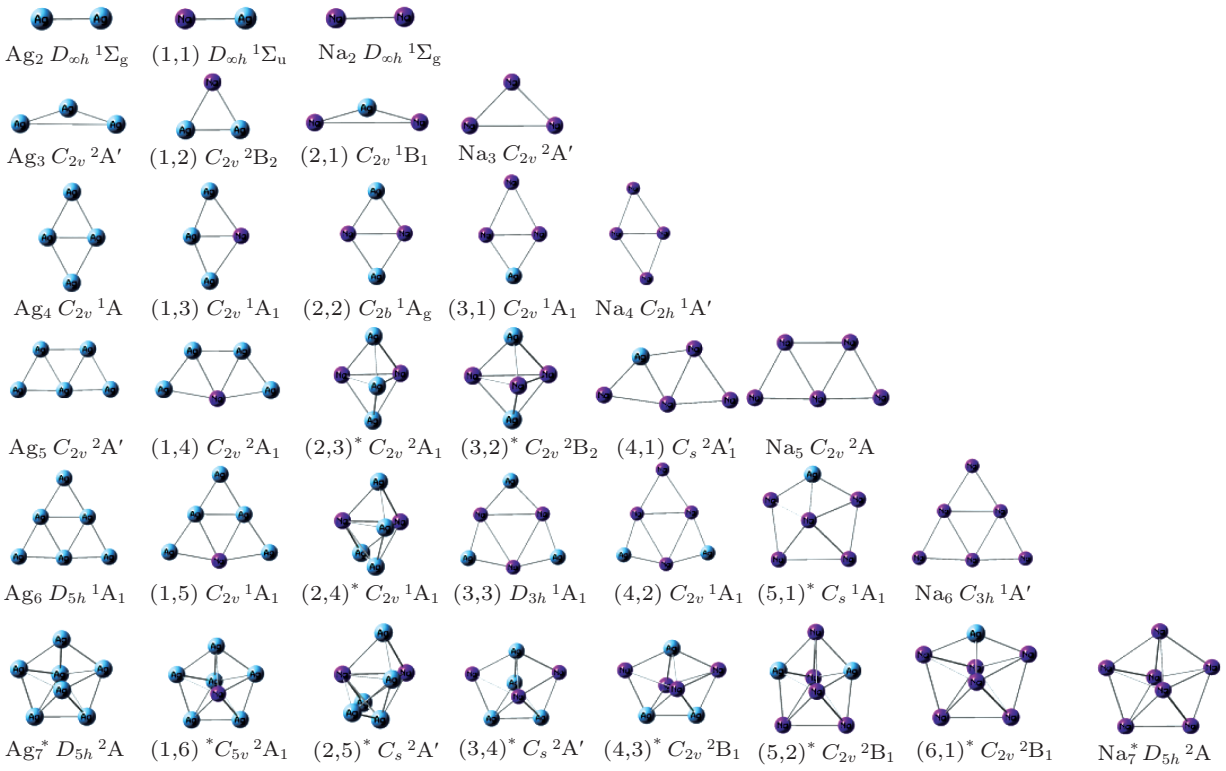


Fig. 1. (colour online) Optimized ground-state structures of the Na_nAg_m ($n+m \leq 7$) clusters and the lowest-energy structures of pure silver clusters Ag_n (n = 2–7) and sodium clusters Na_n (n = 2–7), which are on both sides (with the asterisk denoting three-dimensional structures).

In the cases of Na_2Ag and Na_2Ag_2 in the Na_2Ag_m ($m \leq 5$) series, the most stable isomers are generated by replacing two Ag atoms of Ag_3 and Ag_4 clusters with Na atoms, respectively and these two optimized structures have the geometric symmetries: C_{2v} and D_{2h} respectively. While the following Na_2Ag_m ($3 \leq m \leq 5$) clusters tend to add one Ag to Na_2Ag_{m-1} ($3 \leq m \leq 5$), an early 2D→3D structural transition occurs at Na_2Ag_3. Regarding Na_3Ag_m ($1 \leq m \leq 4$) clusters, the growth pattern of the substituting behaviour above remains. That is to say, substituting one, three, and four Ag atoms for Na in pure Na_4, Na_6, Na_7 clusters, respectively, we obtain the ground-state structures of Na_3Ag, Na_3Ag_3, Na_3Ag_4. With re-

gard to the 3D trigonal bipyramid Na_3Ag_2 cluster, it can be obtained by replacing one Ag atom of Na_2Ag_3. Furthermore, an interesting 2D-to-3D conversion phenomenon appears in the bimetallic Na_3Ag_m clusters. Replacing Na atom in pure Na_n ($5 \leq n \leq 7$) clusters by one, two, three Ag atoms, respectively, the most stable isomers of the Na_4Ag_m ($1 \leq m \leq 3$) clusters are yielded. Besides, the lowest-energy structures of Na_4Ag_m clusters appear to keep similar geometries and growth behaviours to those of pure Na_n ($5 \leq n \leq 7$) clusters. In this way, the 3D pentagon bipyramid isomers Na_5Ag_2 and Na_6Ag are also substituted-Na_7 structures.

Looking through all the optimized structures of Na_nAg_m ($n+m \leq 7$), we can reach the conclusion that for the lowest-energy isomers of Na_nAg_m, an Ag atom in $Na_{n-1}Ag_{m+1}$ cluster is substituted by an Na atom and an Ag cap atom is added onto Na_mAg_{m-1} cluster, thus yielding the dominant growing patterns. In addition, the frameworks of the lowest-energy Na_nAg_m clusters are found to be mostly similar to those of pure sodium and silver clusters.

3.1.2. Geometries and growth pattern behaviors of Li_nAg_m ($n+m \leq 7$)

The lowest-energy structures of Li_nAg_m ($n+m \leq 7$) are obtained and presented in Fig. 2.

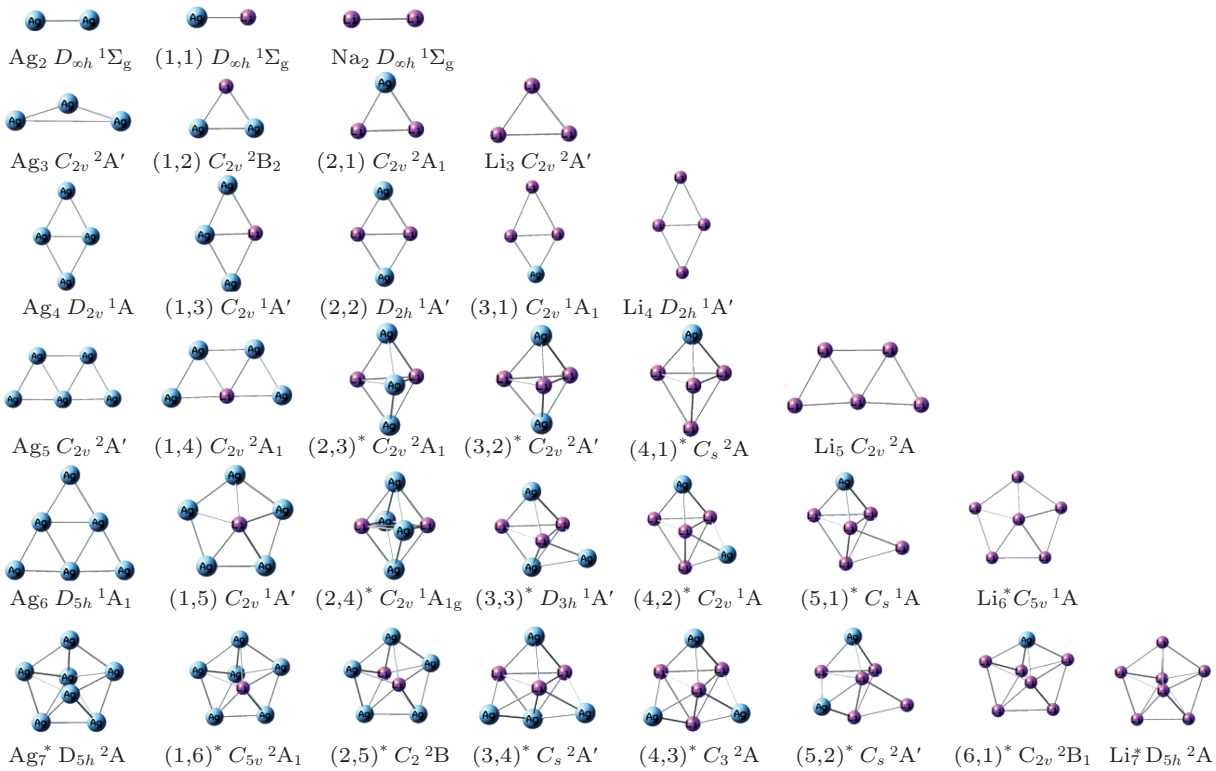


Fig. 2. (colour online) The optimized ground-state structures of the Li_nAg_m ($n+m \leq 7$) clusters, and the lowest-energy structures of pure silver clusters Ag_n ($n = 2$–7) and lithium clusters Li_n, which are on both sides (with asterisk denoting 3D structures).

From Fig. 2, the structures of $LiAg_m$ ($m \leq 6$) clusters generally keep the same frameworks as the corresponding silver clusters, and their features are similar to the optimized configurations of $NaAg_m$ clusters. In the case of small $LiAg_m$ clusters, the biatomic $D_{\infty h}$ LiAg cluster with electronic state $^1\Sigma_g$ is the most stable isomer, whose Li–Ag bond length (2.37 Å) is slightly shorter than the Na–Ag bond length (2.67 Å); and the ground-state structure $LiAg_2$ ($^2B_2$) with C_{2v} symmetry forms an acute isosceles triangle with two identical Li–Ag bonds (2.51 Å) and one Ag–Ag bond (2.78 Å). Concerning Li_2Ag_m ($1 \leq m \leq 5$) clusters shown in Fig. 2, an early structural transition from 2D to 3D also appears at $m = 3$. The geometries of Li_2Ag_m are obtained with Ag-substituted-into $LiAg_{m+1}$ and Ag-capped Li_2Ag_{m-1} structures, which

are similar to the construction forms of Na-doped systems. Specifically, the 2D ground-state Li_2Ag and Li_2Ag_2 isomers are generated with one Ag atom substituted into the optimized geometry of $LiAg_2$ and another Ag atom substituted into the optimized geometry of $LiAg_3$. As for the most stable Li_2Ag cluster, the optimized Li–Ag and Li–Li bond lengths are 2.57 Å and 2.70 Å, respectively, and the angle of Li–Ag–Li is 63.47°, which are all smaller than those of the Na_2Ag cluster. Furthermore, similar calculation results are also found in Li_2Ag_2. As for Li_3Ag_m ($1 \leq m \leq 4$) clusters, we can find an obviously structural conversion from 2D to 3D since $m = 2$. With one Li atom of Li_4 replaced by Ag, a 2D ground-state Li_3Ag (C_{2v}) cluster is produced, and the 3D triangle bipyramid Li_3Ag_2 (C_{2v}) is yielded by substituting Li for one Ag atom in the Li_2Ag_3 cluster. In the light of the optimized Li_3Ag_2, the following 3D lowest-energy Li_3Ag_3 (D_{3h}) and Li_3Ag_4 (C_s) clusters are obtained by capping one atom and two Ag atoms on the surface of Li_3Ag_2, respectively and the most stable Li_4Ag_m and Li_5Ag_m systems yielded by replacing one atom and two Ag atoms in Li_3Ag_m clusters respectively. With one Ag atom substituting one of the different positions of the ground-state structure of the Li_7 cluster, the 3D pentagon bipyramid isomer Li_6Ag is obtained. Moreover, from the above description for Li_3Ag_m, Li_4Ag_m, and Li_5Ag_m systems it follows that the extra Ag atom tends to form the maximum number of Li–Ag bonds. This distinctive phenomenon may be related to the atomic average binding energy E_b (LiAg) > E_b (Ag_2) which is shown in Fig. 3. Namely, for the larger Li–Ag clusters, the maximum Li–Ag bonds and compact 3D geometries are formed due to the stronger interaction between Li and Ag.

In a similar way to the building progress of Na_nAg_m clusters, we can perceive clearly from Fig. 2 that the primary growth patterns are due to replacing an Ag atom in $Li_{n-1}Ag_{m+1}$ and Ag-capped Li_nAg_{m-1} clusters. In addition, for the most stable isomers of larger binary Li–Ag clusters, the optimized 3D geometric forms are distinct from their corresponding 2D bare Ag_n or Li_n clusters, that is, the triangular bipyramid form is found to be the main subunit.

3.2. Size dependence of relative stability

In order to obtain the detailed information about the relative stabilities and different-sized physical properties of clusters, we perform some calculations of the atomic average binding energy E_b, fragmentation energy $\Delta_1 E$, and second-order difference of energy $\Delta_2 E$. For pure N_n (N=Ag, Na, Li, $n \leq 7$) and M_nAg_m clusters, the corresponding E_b, $\Delta_1 E$, and $\Delta_2 E$ are defined as follows:

$$\begin{aligned} E_b &= [(nE(N) - E(N_n)]/n, \\ \Delta_1 E &= E(N_{n-1}) + E(N) - E(N_n), \\ \Delta_2 E &= E(N_{n-1}) + E(N_{n+1}) - 2E(N_n), \end{aligned} \quad (1)$$

and

$$\begin{aligned} E_b &= [nE(M) + mE(\mathrm{Ag}) - E(M_nAg_m)]/(n+m), \\ \Delta_1 E &= E(M_nAg_{m-1}) + E(\mathrm{Ag}) - E(M_nAg_m), \\ \Delta_2 E &= E(M_nAg_{m-1}) + E(M_nAg_{m+1}) \\ &\quad - 2E(M_nAg_m), \end{aligned} \quad (2)$$

where $E(N)$, $E(N_n)$, $E(N_{n-1})$, $E(N_{n+1})$, $E(M)$, $E(\mathrm{Ag})$, $E(M_nAg_m)$, $E(M_nAg_{m-1})$, and $E(M_nAg_{m+1})$ denote the total energies of the most stable isomers for N, N_n, N_{n-1}, N_{n+1}, M, Ag, M_nAg_m, M_nAg_{m-1}, M_nAg_{m+1} clusters, respectively. The calculated values of E_b, $\Delta_1 E$, and $\Delta_2 E$ of the most stable Ag_n, Na_n, Li_n, and M_nAg_m clusters with respect to cluster size are respectively plotted in Figs. 3, 4, and 5. Meanwhile, with the total number n arising from 2 to 7, the average binding energies of bare Ag_n, Na_n, and Li_n clusters each have an increasing tendency. Besides, the data exhibit a sequence as E_b (Ag_n) > E_b (Li_n) > E_b (Na_n) for identical cluster size n, which hints that Ag_n clusters have higher stability than Li_n and Na_n clusters. It is worth pointing out that this result is in good agreement with the available experimental results of dissociation energies $D_e(Ag_2) > D_e$ (Li_2) > D_e (Na_2).[24,25] Further, similar to the mutative pattern of pure Ag_n, Na_n, and Li_n clusters, the binding energies of bimetallic M_nAg_m clusters each have an overall rising tendency as Ag atom m increases, indicating that adding the Ag atoms enhances the stabilities of the Na_n and Li_n frameworks for each series of Na_nAg_m and Li_nAg_m ($n + m \leq 7$) clusters.

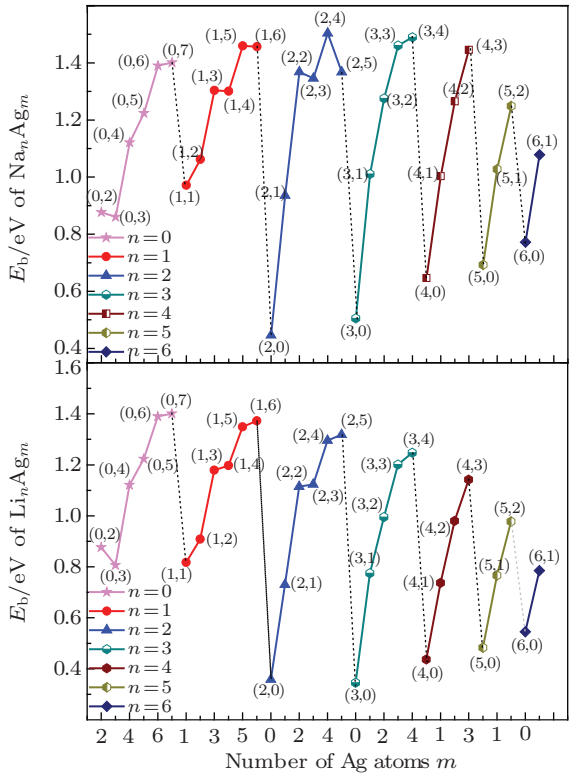


Fig. 3. (colour online) Size dependences of the atomic average binding energy E_b for the most stable Ag_n, Na_n, Li_n, and M_nAg_m (M=Na, Li; $n+m \leq 7$) clusters.

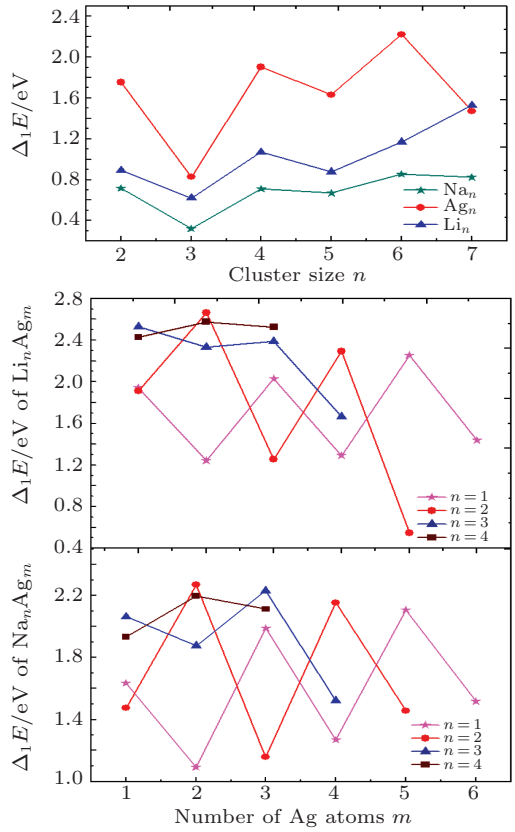


Fig. 4. (colour online) Size dependences of the fragmentation energy Δ_1E for the most stable Ag_n, Na_n, Li_n, and M_nAg_m (M=Na, Li; $n+m \leq 7$) clusters.

In cluster physics, the fragmentation energy Δ_1E is viewed as a significant parameter to reflect the relative stability of the cluster. The size-dependent fragmentation energies of pure Ag_n, Na_n, and Li_n ($n \leq 7$) as well as M_nAg_m (M=Na, Li; $n+m \leq 7$) clusters are investigated and described in Fig. 4. For pure clusters, one can note that the fragmentation energies each exhibit a pronounced odd–even alternative behaviour as a function of cluster size n. The study also shows a visible sequence as Δ_1E (Ag_n) > Δ_1E (Li_n) > Δ_1E (Na_n). Meanwhile, a similar odd–even oscillation phenomenon occurs to those of M_nAg_m clusters, and the peaks are located at $MAg_{1,3,5}$, $M_2Ag_{2,4}$, $M_3Ag_{1,3}$, M_4Ag_2 respectively. All in all, according to the above analyses, we can clearly conclude that for the ground-state pure Ag_n, Na_n, Li_n, and M_nAg_m, the clusters with even-numbered total atoms exhibit a higher stability than the others.

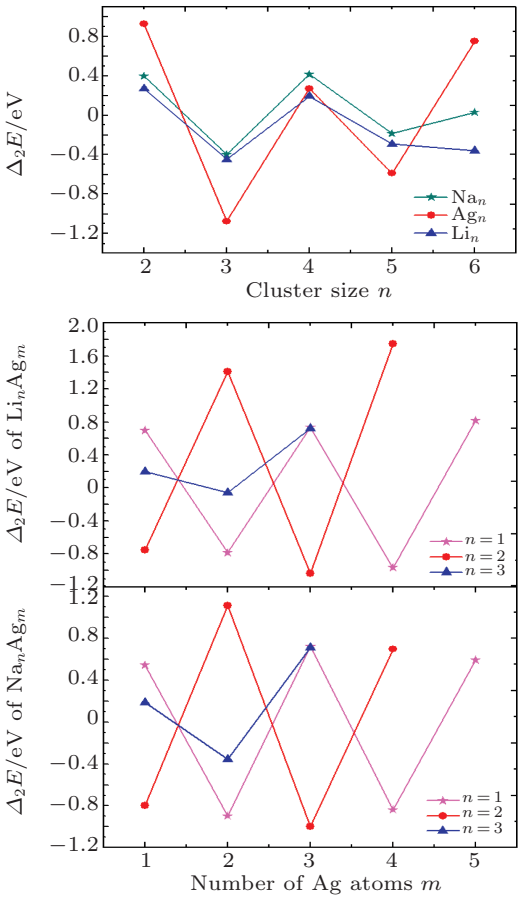


Fig. 5. (colour online) Size dependences of the second-order difference of energy Δ_2E for the most stable Ag_n, Na_n, Li_n, and M_nAg_m (M=Na, Li; $n+m \leq 7$) clusters.

The second-order difference of energy Δ_2E of the clusters is also taken into account to further explore

their relative stabilities at various sizes. The calculated results are shown in Fig. 5. For pure and doped clusters, the curves of $\Delta_2 E$ also each present a similar oscillatory behaviour along with the cluster size. Moreover, the $\Delta_2 E$ values of $Ag_{2,6}$ are found to be larger than those of $Na_{2,6}$ and $Li_{2,6}$, and the $\Delta_2 E$ of $Ag_{3,5}$ appear to be lower than any of $M_{3,5}$ (M=Na, Li) clusters, while Ag_4 has a middle $\Delta_2 E$ value.

3.3. HOMO–LUMO energy gaps

The energy gap between the highest occupied molecular orbital (HOMO) and the lowest unoccupied molecular orbital (LUMO) is considered to be another powerful parameter that reflects the ability of electrons to jump from the occupied orbital to the unoccupied orbital. Explicitly, clusters with the larger HOMO–LUMO gaps are less reactive and possess relatively higher stability. The corresponding HOMO–LUMO energy gaps for pure Ag_n, Na_n, Li_n, and M_nAg_m (M=Na, Li) clusters are plotted in Fig. 6.

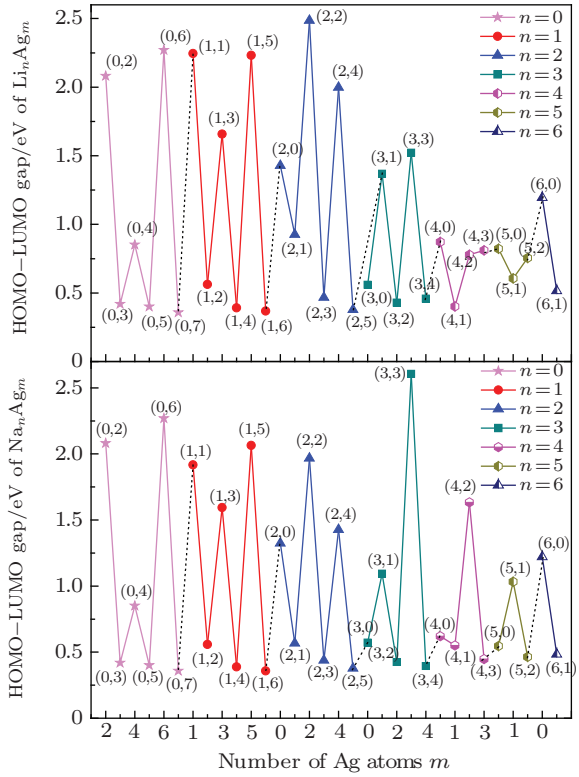


Fig. 6. (colour online) Size dependences of the HOMO–LUMO energy gaps for the most stable Ag_n, Na_n, Li_n, and M_nAg_m (M=Na, Li; $n+m \leq 7$) clusters.

It can be seen that their HOMO–LUMO gaps each have an oscillating phenomenon just like their corresponding fragmentation energies and the second-order difference of energies. This indicates that pure $Ag_{2,4,6}$, $Na_{2,4,6}$, $Li_{2,4,6}$, and $MAg_{1,3,5}$, $M_2Ag_{2,4}$, $M_3Ag_{1,3}$, M_4Ag_2 (M=Na, Li) clusters each with even-numbered total atoms have larger HOMO–LUMO gaps and weaker chemical activity than their neighbouring clusters. Since the Ag atom possesses an s valence electron outside its closed d shell, which is similar to s-only electron of alkali metal, it can be concluded that the cluster with higher stability is dominated by even-numbered valence electrons due to their closed-shell electronic configuration.

3.4. Electronic properties

It is known that ionization potential and electron affinity have proved to be important properties to study the changes in electronic structures of the clusters with different sizes. Assuming that the ground-state geometries of the charged clusters are the same as those of the neutral clusters, the calculated quantities are known as the vertical ionization potential (VIP) and vertical electron affinity (VEA), which are defined as the following formulas:

$$\begin{aligned} \mathrm{VIP} &= E_{(\text{cation at optimized neutral geometry})} \\ &\quad - E_{(\text{optimized neutral})}, \\ \mathrm{VEA} &= E_{(\text{optimized neutral})} \\ &\quad - E_{(\text{anion at optimized neutral geometry})}. \end{aligned} \tag{3}$$

Besides, chemical hardness (η) is established as an electronic quantity which is used to characterize the relative stabilities of molecules and aggregates through the principle of maximum hardness proposed by Pearson.[38] Based on the above calculations, the corresponding chemical hardness is also calculated, which is defined as

$$\eta = (\mathrm{VIP} - \mathrm{VEA}). \tag{4}$$

The calculated values of chemical hardness with respect to the cluster size for the pure and bimetallic clusters are plotted in Fig. 7. As can be seen in Fig. 7, the curves of pure and M_nAg_m clusters both show typical oscillating behaviours as cluster size increases, indicating that the clusters $Ag_{2,4,6}$, $Na_{2,4,6}$, $Li_{2,4,6}$, and $MAg_{1,3,5}$, $M_2Ag_{2,4}$, M_3Ag_3, M_4Ag_2 (M=Na, Li) with higher hardness values are more stable than their neighbouring clusters. Further, the maximum peaks are located at Ag_2, Na_6, Li_6, and MAg, M_2Ag_2,

M_3Ag_3, M_4Ag_2 (M=Na, Li), respectively. In other words, clusters with 2, 4, and 6 electrons have particular higher chemical stabilities than their neighbouring clusters. This feature is in good accordance with the above results of fragmentation energies, second-order difference of energies, HOMO–LUMO energy gaps, and vertical ionization potential.

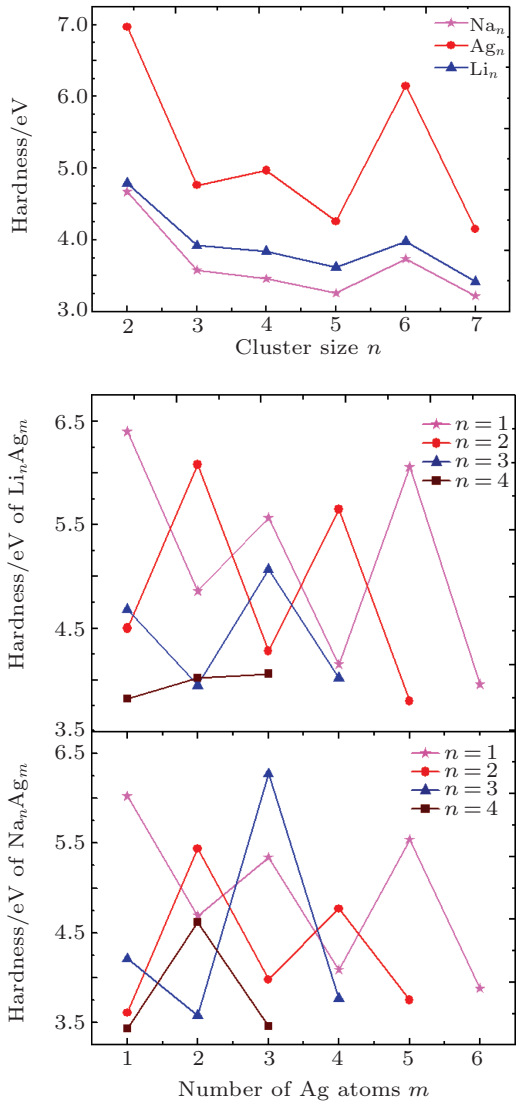


Fig. 7. (colour online) Size dependences of the chemical hardnesses for the most stable Ag_n, Na_n, Li_n, and M_nAg_m (M=Na, Li; $n+m \leq 7$) clusters.

4. Conclusions

By using the first-principle density functional theory at BP86/GENECP (LanL2DZ for the Ag atom and 6-311G* for the Na/Li atom) level, the geometric structures, relative stabilities, and electronic properties of mixed M_nAg_m (M=Na, Li; $2 \leq n+m \leq 7$) clusters as well as pure Ag_n, Na_n, Li_n ($n \leq 7$) systems are systematically studied in this work. The conclusions drawn from the present study are summarized as follows.

(i) A large number of initial configurations are optimized to obtain the most stable clusters for Ag_n, Na_n, Li_n, and M_nAg_m clusters. The optimized results reveal that all the lowest-energy isomers of pure and bimetal M_nAg_m clusters prefer to have the lowest spin multiplicity. Moreover, Ag_n, Na_n ($n \leq 7$) clusters tend to be 2D structures until $n = 7$, while earlier transitions from 2D to 3D arise at Li_6 for Li_n clusters. In contrast, the first 3D structures are observed early at $n + m = 5$ for both Na_nAg_m and Li_nAg_m cluters. In the case of M_nAg_m clusters, the dominant growth patterns are one M-substituted $M_{n-1}Ag_{m+1}$ and Ag-capped M_nAg_{m-1} structures.

(ii) The relative stabilities of the investigated clusters are studied in terms of the atomic average binding energies, the fragmentation energies, the second-order difference energies, and the HOMO–LUMO energy gaps. The most stable Ag_n, Na_n, Li_n, and M_nAg_m clusters exhibit a similar odd–even alternation phenomenon along with the cluster size. According to our analysis, we should point out that in different series, the clusters with closed electronic shells including $Ag_{2,4,6}$, $Na_{2,4,6}$, $Li_{2,4,6}$, and $MAg_{1,3,5}$, $M_2Ag_{2,4}$, M_3Ag_3, M_4Ag_2 (M=Na, Li) have higher stabilities than their neighbouring ones.

(iii) Based on the analysis of chemical hardness, a visible oscillatory behaviour is observed as cluster size increases. In particular, the clusters Ag_2, Na_6, Li_6, and MAg, M_2Ag_2, M_3Ag_3, M_4Ag_2 (M=Na, Li) have the maximum peaks among corresponding series, indicating that the clusters with even-numbered (2, 4, 6) closed electronic shells have obvious chemical stabilities.

References

[1] Downes A and Dumas P 2003 *Appl. Surf. Sci.* **212** 770
[2] Graciani J, Oviedo J and Sanz J F 2006 *J. Phys. Chem.* B **110** 11600
[3] Liu Q, Cheng X L, Li D H and Yang Z J 2011 *Acta Phys. Sin.* **59** 8829 (in Chinese)
[4] Häkkinen H, Abbet S, Sanchez A, Heiz U and Landman U 2003 *Angew. Chem. Int. Ed.* **42** 1297
[5] Chen Y T, Ho T H, Lim C S and Lim B H 2010 *Chin. Phys.* B **19** 118105
[6] Yuan D W, Gong X G and Wu R Q 2008 *Phys. Rev.* B **78** 035441

[7] Zhang X R, Wu L Q and Rao Q 2011 *Acta Phys. Sin.* **60** 083601 (in Chinese)
[8] Yuan D W, Wang Y and Zeng Z 2005 *J. Chem. Phys.* **122** 114310
[9] Brack M 1993 *Rev. Mod. Phys.* **65** 677
[10] An Y P, Yang C L, Wang M S, Ma X G and Wang D H 2010 *Chin. Phys.* B **19** 113402
[11] Shi G S, Wang Z G, Zhao J J, Hu J and Fang H P 2011 *Chin. Phys.* B **20** 068101
[12] Zhang S H, An H L, Liu Y Z, Zhang Z D, Geng J P and Zhang Y 2011 *Acta Phys. Sin.* **60** 048701 (in Chinese)
[13] Bowlan J, Liang A and de Heer W A 2011 *Phys. Rev. Lett.* **106** 043401
[14] Zhang J C, Sun J F and Liu Y F 2011 *Chin. Phys.* B **20** 023401
[15] Li X M, Han H L and He G P 2011 *Acta Phys. Sin.* **60** 087014 (in Chinese)
[16] Hristova E, Grigoryan V G and Springborg M 2009 *Eur. Phys. J.* D **52** 35
[17] Baletto F and Ferrando R 2005 *Rev. Mod. Phys.* **77** 371
[18] de Heer W A 1993 *Rev. Mod. Phys.* **65** 611
[19] Choi Y C, Lee H M, Kim W Y, Kwon S K, Nautiyal T, Cheng D Y, Vishwanathan K and Kim K S 2007 *Phys. Rev. Lett.* **98** 076101
[20] Jena N K, Chandrakumar K R S and Ghosh S K 2009 *J. Phys. Chem.* C **113** 17885
[21] Gonella F, Caccavale F, Bogomolova L D and Quaranta A 1998 *J. Appl. Phys.* **83** 1200
[22] Ge G X, Jing Q, Cao H B, Yang Z Q, Tang G H and Yang H X 2011 *Acta Phys. Sin.* **60** 103102 (in Chinese)
[23] Li Y F, Kuang X Y, Wang S J, Li Y and Zhao Y R 2011 *Phys. Lett.* A **375** 1877
[24] Brock L R, Knight A M, Pilgrim J S and Duncan M A 1997 *J. Chem. Phys.* **106** 6268
[25] Stangassinger A, Knight A M and Duncan M A 1997 *Chem. Phys. Lett.* **266** 189
[26] Rodriguez J A and Hrbek J 1994 *J. Phys. Chem.* **98** 4061
[27] Wannere C S, Corminboeuf C, Wang Z X, Wodrich M D, King R B and Schleyer P R 2005 *J. Am. Chem. Soc.* **127** 5701
[28] Tellgren E, Henriksson J and Norman P 2007 *J. Chem. Phys.* **126** 064313
[29] Lin Y C, Sundholm D, Jusélius J, Cui L F, Li X, Zhai H J and Wang L S 2006 *J. Phys. Chem.* A **110** 4244
[30] Baruah T, Blundell S A and Zope R R 2001 *Phys. Rev.* A **64** 043202
[31] Becke A D1988 *Phys. Rev.* A **38** 3098
[32] Perdew J P 1986 *Phys. Rev.* B **33** 8822
[33] Hay P J and Wadt W R 1985 *J. Chem. Phys.* **82** 270
[34] Wadt W R and Hay P J 1985 *J. Chem. Phys.* **82** 284
[35] Hay P J and Walt W R 1985 *J. Chem. Phys.* **82** 299
[36] Frisch M J, Trucks G W, Schlegel H B, Scuseria G E *et al.* 2004 *Gaussian* 03, Revision E.01 (Wallingford CT: Gaussian, Inc)
[37] Koutecký V B, Češpiva L, Fantucci P and Koutecký J 1993 *J. Chem. Phys.* **98** 7981
[38] Pearson R G 1997 *Chemical Hardness: Applications from Molecules to Solids* (Weinheim: Wiley-VCH)